Influence of Intermolecular Interactions on the Mössbauer Quadrupole Splitting of Organotin(IV) Compounds as Studied by DFT Calculations

ARTICLE *in* THE JOURNAL OF PHYSICAL CHEMISTRY A · JANUARY 2008

Impact Factor: 2.69 · DOI: 10.1021/jp075628b · Source: PubMed

5 AUTHORS, INCLUDING:

Szilvia Karpati
French National Centre for Scientific Research
11 PUBLICATIONS **226** CITATIONS
SEE PROFILE

Roland Szalay
Eötvös Loránd University
9 PUBLICATIONS **34** CITATIONS
SEE PROFILE

Attila Csaszar
Eötvös Loránd University
197 PUBLICATIONS **5,708** CITATIONS
SEE PROFILE

Influence of Intermolecular Interactions on the Mössbauer Quadrupole Splitting of Organotin(IV) Compounds as Studied by DFT Calculations

Szilvia Kárpáti,*,† Roland Szalay,‡ Attila G. Császár,§ Károly Süvegh,† and Sándor Nagy†

Institute of Chemistry, Eötvös Loránd University, 1518 Budapest 112, P.O. Box 32, Hungary

Received: July 18, 2007; In Final Form: September 23, 2007

The influence of intermolecular interactions on the Mössbauer quadrupole splitting (Δ) of ^{119}Sn was investigated in detail by density functional theory (DFT) calculations. Six organotin(IV) complexes [$Me_2Sn(acac)_2$ (**1**), Ph_3SnCl (**2**), Me_3Sn-succinimide (**3**), Me_3Sn-phthalimide (**4**), Me_3SnCl (**5**), and $cHex_3SnCl$ (**6**)] of known solid-state structures and quadrupole splittings were selected. Theoretical Δ values were calculated for both fully optimized geometries and experimental solid-state structures of different size, and the results were compared to the experimental Δ values. Compared to a synthetic procedure described in the literature for compound **4**, a more convenient synthesis is reported here. The experimental Δ of this compound has also been redetermined at 80 K. For compounds with negligible intermolecular interactions in the solid state, calculated Δ values obtained did not vary significantly. In contrast, the calculated Δ values turned out to be very sensitive to the size of the supramolecular moiety considered in the crystal lattice. The crystal structure of compound **2** shows no significant intermolecular interactions; however, the calculated and the experimental Δ values remained very different, even when the supramolecular moiety considered was extended. Distortion of the coordination sphere of tin in the molecule of **2** toward a trigonal bipyramidal geometry was considered, and a possible weak intermolecular Sn···Cl interaction was included in the model. Steps of the distortion followed the new structure correlation function, which was found for the R_3SnCl (R = alkyl, aryl) compounds. The experimental Δ value could be approached by this method. These results suggest that compound **2** is involved in some unexpected intermolecular interaction at 80 K.

1. Introduction

The nuclear quadrupole splitting energy, ΔE_Q, is a spectroscopic characteristic of the energy of interaction between the nuclear quadrupole moment, Q, of a given nucleus with the electric field gradient (EFG) created by the charge density surrounding it. The EFG is represented by a diagonal and traceless tensor **V**, whose eigenvalues, V_{xx}, V_{yy}, and V_{zz}, satisfy the conventional choice

$$|V_{zz}| \geq |V_{yy}| \geq |V_{xx}| \tag{1}$$

In the case of $I = {}^3/_2 \rightarrow {}^1/_2$ nuclear transitions, as with ^{57}Fe or ^{119}Sn, ΔE_Q is related to the principal components of $\boldsymbol{V}$ by the expression

$$\Delta E_Q = \frac{1}{2} eQV \tag{2}$$

where e is the elementary charge, and V is defined as

$$V = V_{zz}\sqrt{1 + \frac{\eta^2}{3}} \tag{3}$$

η is the conventional asymmetry parameter characterizing **V**:

$$\eta = \frac{V_{xx} - V_{yy}}{V_{zz}} \tag{4}$$

The nuclear quadrupole splitting energy is proportional to an experimental quantity called quadrupole splitting (Δ) in Mössbauer spectroscopy,

$$\Delta \propto \Delta E_Q \tag{5}$$

The value of Δ is given in velocity units (e.g., in mm s^{-1}), and the conversion between Δ and ΔE_Q is given explicitly in eq 6 of section 2.2.

The purpose of measuring Δ is to extract information on the local structure surrounding the nucleus. Since the EFG depends strongly on the electronic environment of the nucleus considered, a dependable calculation of V can provide a useful tool to interpret the measured Δ and to suggest a solid-state structure of the compound considered. Hence, the determination of accurate EFG values by theoretical methods is an active and challenging field of research.

For a long time, a simple point-charge model was widely used to interpret experimental Mössbauer spectroscopic results.[1−3] While on the basis of empirical parameters, these predictions often deviated significantly from the experimental values. Later on, advances in electronic structure theory permitted the development of several ab initio methods to calculate the EFG, providing a physical interpretation of the measured quadrupole splittings (see, for example, ref 4 for tin compounds). For accurate calculation of the EFG, correlated motion of the electrons has to be considered and fairly large atom-centered Gaussian basis sets need to be applied.[5] These requirements limit severely the size of the molecules that can be investigated. Gerber and co-workers[6] argued that similarly to many other applications of electronic structure theory, it is sufficient to use a locally dense basis set, so that the use of a large basis is only

* To whom correspondence should be addressed. E-mail: karpati@chem.elte.hu.
† Laboratory of Nuclear Chemistry.
‡ Laboratory of Organosilicon Chemistry.
§ Laboratory of Molecular Spectroscopy.

10.1021/jp075628b CCC: $37.00
Published on Web 11/13/2007

TABLE 1: Calculated *V* Values (See Eq 3), Obtained for the in Vacuo and the Solid-State Crystal Structures (XRD Monomer) of Compounds 1−5, Together with Calculated and Experimental Quadrupole Splittings (Δ_{calc} and Δ_{exp})

	in vacuo structure (optimized geometry)		XRD monomer[a] (without optimization)		
compound	V_{calc}	Δ_{calc}[c]	V_{calc}	Δ_{calc}[c]	Δ_{exp}[b]
1	4.25[d]	3.95[d]	4.30	3.99	4.02[e] (3.93[f])
2	−1.83	−1.70	−2.00	−1.86	(−)2.61[g]
3	−2.62	−2.44	−3.11	−2.89	(−)3.14[h] (3.35[i])
4	−2.58	−2.40	−2.83	−2.63	(−)2.92[j] (3.22[i])
5	−2.33	−2.17	−2.71	−2.52	(−)3.32[k]

[a] Structure corresponding to the results of the X-ray diffraction analysis. [b] The values given in parentheses are other literature values. [c] For the calculation at DFT(B3LYP) level (for details, see section 2.2) of the quadrupole splittings (Δ in mm s^{-1}) from the value of V (in au), the calibration curve proposed by Barone et al.[9] was used (with the calibration factor 0.93 mm s^{-1} au^{-1}). [d] Theoretical values found by other authors are $V_{nonrel} = 4.60$ au ($\Delta_{calc} = 4.27$ mm s^{-1}) at the nonrelativistic level[9] and $V_{rel} = 5.69$ au ($\Delta_{calc} = 4.13$ mm s^{-1}) at the relativistic level.[12] [e] From ref 17. [f] From ref 18. [g] From ref 19. [h] From ref 20. [i] From ref 21. [j] The present work. [k] From ref 22.

TABLE 2: Different Quadrupole Moment Values (*Q*) of the ^{119}Sn Nucleus Found in the Literature and the Calibration Factors ($^1/_2eQc/E_0$) Calculated from Them

designation of Q[a]	Q[b]	$^1/_2eQc/E_0$[c]
Q_{exp}	10.9 ± 0.8[d]	0.666
Q_1	11.9 ± 0.1[e]	0.727
Q_2	12.8 ± 0.7[f]	0.782
Q_3	15.2 ± 4.4[g]	0.929

[a] Q_{exp} of the tin nucleus has been determined by experiment (Mössbauer spectroscopy); Q_1 and Q_3 were obtained by relativistic and nonrelativistic DFT(B3LYP) methods; and the full-potential linear-muffin-tin-orbitals (FP-LMTO) method within the local-density approximation (LDA) to DFT was used for Q_2. [b] Literature values of the nuclear quadrupole moment (Q) given in fm^2. [c] The calibration factor $^1/_2eQc/E_0$ (mm s^{-1} au^{-1}) is the proportionality constant between the quadrupole splitting (Δ) and V (see eq 2). For the calculation of this constant, see section 2.2. [d] From ref 23. [e] From ref 9. [f] From ref 4a. [g] From ref 12.

necessary for the description of the atom that contains the nucleus of interest, while on the rest of the atoms much smaller basis sets can be placed without really sacrificing accuracy. An alternative to ab initio calculations is the use of density functional theory (DFT) techniques, since they can provide accurate results for many physical properties at reasonably low computational cost. Starting from 1997, simple DFT has been successfully applied to the calculation of EFGs;[7] however, hybrid DFT methods seem to be even more accurate.[8] Using one of these methods, Barone et al.[9] have recently established a calibration function from a linear regression analysis of the correlation of the experimental Δ values with the corresponding calculated V values for 34 tin compounds. Their calculations of V values have been performed on geometries fully optimized at the DFT(B3LYP)[10] level employing the all-electron DZVP basis set.[11] In a follow-up study, Krogh et al.[12] have computed the EFG at the scalar relativistic DFT(B3LYP) level for the same 34 compounds. The calibration obtained with relativistic corrections yields a value for Q which is in good agreement with the experimental value (see Table 2).

Barone et al.[9] considered only tin compounds composed of monomers (without significant intermolecular interactions) to minimize the differences between the in vacuo and the solid-state structures. However, in numerous compounds, packing effects in the crystal lattice influence the coordination sphere of tin so that the measured Δ is very different from the value obtained for the gas-phase structure. The present investigation provides a further example of the applicability of the DFT-(B3LYP) method to determine the EFG, but now, in contrast to previous studies on this subject, the emphasis is shifted toward the influence of solid-state environmental effects.

2. Experimental and Computational Methods

2.1. Synthesis and Characterization of *N*-(Trimethylstannyl)phthalimide (4). Compound **4** was prepared in this study by a method different from that published earlier.[13] All operations were carried out under moisture-free conditions. A solution of trimethyltin chloride (4.27 g, 21 mmol) in anhydrous THF (20 mL) was added dropwise to a suspension of potassium phthalimide (3.91 g, 21 mmol) in 30 mL THF. The mixture was then stirred at ambient temperature under nitrogen for 8 h. The precipitated potassium chloride was filtered off and the solvent was evaporated in vacuo to give 5.0 g of a white crude product (75%). The solid residue was subsequently purified by vacuum sublimation. ^{1}H NMR (TMS in $CDCl_3$, δ, ppm): 0.7 (t, 9H, $SnMe_3$); 7.7 (m, 4H, aromatic ring). ^{13}C NMR: ($CDCl_3$, δ, ppm): −4.5 (3C, $SnMe_3$); 122.5 and 133.2 (phthalimido ligand, ring); 176.3 (2C, C═O). *m*/*z* (%): 296 (M-15), 266 (M-45), 252, 222, 147 (phthalimido ligand), 104 ($C_6H_4CO^+$), 76 ($C_6H_4^+$). Mössbauer parameters (mm s^{-1}): IS (isomer shift, δ) = 1.41 ± 0.01, QS (quadrupole splitting, Δ) = 2.92 ± 0.03. Elemental analysis calcd. (%) for $C_{11}H_{13}NO_2Sn$ (309.92): C 42.59, H 4.19, N 4.52. Found: C 43.72, H 3.86, N 4.50.

2.2. Theoretical Calculations. The present study is based upon the assumption that the computational errors introduced because of the neglect of relativistic effects, the use of a density functional theory (DFT) approach, and the use of a finite basis set are basically compensated by the calibration process employed (see eqs 2 and 6). The studies of Krogh et al.[12] and Barone et al.[9] proved the suitability of the DFT(B3LYP) approach for the task of determining correct EFG values for a large set of organotin compounds. The effect of special relativity on EFG computations for organotin compounds has been considered by Krogh et al.[12] at the DFT(B3LYP) level and was found to be important basically to improve the correlation of the computed nuclear quadrupole splitting energies with the experimental quadrupole splittings already existing at the nonrelativistic level. Consequently, if appropriate basis sets are used for the EFG calculations, the results obtained after the calibration process should be accurate enough to establish structural trends in the compounds investigated.

All geometry optimizations and EFG calculations were performed at the nonrelativistic hybrid HF/DFT(B3LYP)[10] level using the Gaussian03W[14] program package. The starting geometries for the optimizations were chosen to be the experimental X-ray geometries determined for each compound. For the ligand atoms C, N, O, H, and Cl, the 6-31+G(d) basis set was used throughout this study.

Effects due to special relativity are of importance for tin and should not be neglected. However, for systems of large size, like the organotin compounds investigated here, all-electron relativistic calculations are rather costly. A simple solution to overcome this problem is offered by the use of relativistic effective core potentials (RECP). Thus, during geometry optimizations, the LanL2DZ[15] basis set has been employed for tin.

As the core electron density of tin plays an important role in the computed quadrupole splitting values, RECPs are not

CHART 1

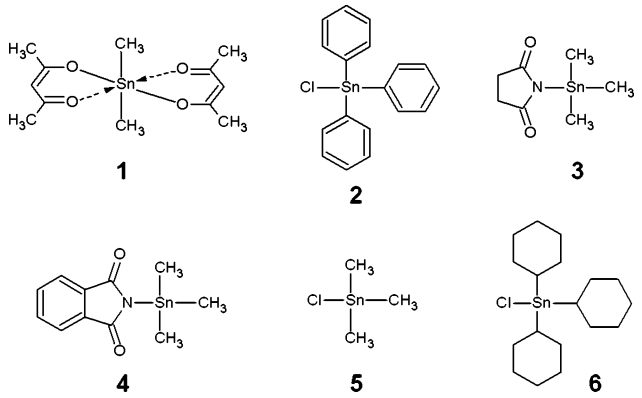

appropriate for the evaluation of this quantity. In fact, an all-electron basis set is essential, so the DGDZVP[11] basis set was used for the computation of the EFG tensor. This basis set does not allow taking relativistic effects into account. The spatial coordinates for these calculations corresponded both to the optimized and the experimental solid-state structures of varying size.

The quantity V was calculated from the computed V_{ii} values according to eq 3. The relation between V and the quadrupole splitting energy, ΔE_Q, is given by eq 2, and the conversion factor ($^1/_2eQ$) depends on the value of the nuclear quadrupole moment (Q). As four different values of Q were found in the literature, the calibration factor ($^1/_2eQc/E_0$) between Δ and V was evaluated in each case (see Table 2). This was based on the Doppler relation as follows:

$$\Delta = (\Delta E_Q/E_0)\cdot c = \left(\frac{1}{2}eQV/E_0\right)\cdot c \qquad (6)$$

where ΔE_Q is the energy difference between the $m_I = {}^3/_2$ and $m_I = {}^1/_2$ sublevels of a given excited-state ($I = {}^3/_2$) ^{119}Sn nucleus in the observed compound and E_0 (23.83 keV) is the energy of the γ radiation emitted by the same ^{119}Sn nucleus when it gets de-excited from the $I = {}^3/_2$ state to its $I = {}^1/_2$ ground state. If V is given in atomic units, then E_0 also has to be converted by using the relations 1 Hartree = 27.2113845 eV and E_0 = 875.7364036 au. The elementary charge, e equals 1 au, and Q are converted to atomic units by using the atomic unit of length, 1 bohr = 0.5291772083 Å.[14]

3. Structures and Quadrupole Splittings

3.1. EFG Calibration. As underlined in the Introduction, an accurate calibration of the calculated EFG would be very helpful during interpretation of experimental values of Mössbauer quadrupole splittings, and hence these data would provide more reliable information on the structure of compounds, even if suitable crystals for X-ray analysis are not available.

Most electronic structure calculations of EFG values employed gas-phase structures. However, this strategy is expected to yield accurate Mössbauer spectroscopic results only for compounds which exhibit no intermolecular interactions in the solid state. In tin compounds, however, intermolecular interactions can be quite important as they lead to significant distortions upon the gas-phase molecular structure.

As the present work was performed to show how the calculated EFGs are affected by intermolecular interactions, five appropriate organotin compounds (**1**−**5**) were selected for this study (Chart 1). (Chart 1 also shows compound **6**, which will be discussed later.) Crystal structures[16] and experimentally

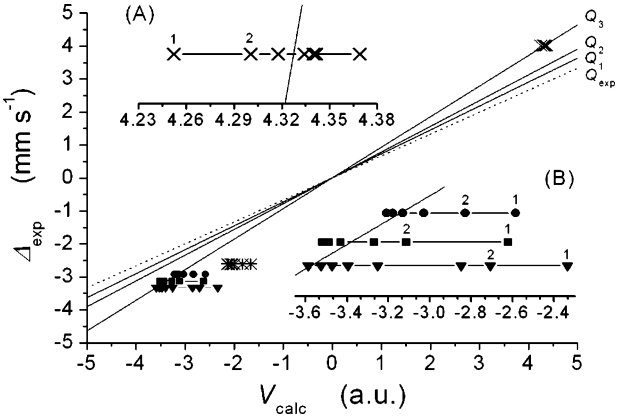

Figure 1. The horizontal lines (enlarged in the inserts) represent experimental quadrupole splitting values (Δ_{exp}) of compounds **1**−**5** versus V_{calc} values, calculated for different supramolecular moieties of each compound. The slanting lines show the four calibration curves calculated from the four different quadrupole moment values (Q) found in the literature (see Table 2). Insert A is an enlargement of the plot for compound **1** (−×−). Insert B is an enlargement of the plots for compounds **3** (−■−), **4** (−●−), and **5** (−▼−). Numbering 1 and 2 above plots in the inserts indicates optimized (in vacuo) and nonoptimized (solid-state) monomers, respectively. Note that all plots, except for that of compound **2** (−∗−), approach the calibration curve obtained from Q_3 as the size of the supramolecular moieties increases (to the left).

determined quadrupole splittings are known for compounds **1**−**5**, and the quadrupole splittings are collected in Table 1.

According to their crystal structure analysis, compounds **1** and **2** exhibit negligible intermolecular interactions. In contrast, the structures of compounds **3**−**5** clearly show the effects of intermolecular interactions. In each case, V was computed for the optimized in vacuo structure as well as at nonoptimized structures taken directly, that is, without reoptimization, from the solid-state crystal structure. The relevant results are collected in Table 1. The absolute value of the difference (δV) between the two values obtained for the monomers, that is, with and without optimization, increases as the strength of the intermolecular forces increases. For example, $\delta V = 0.05$ au for **1** with negligible intermolecular interaction, $\delta V = 0.25$ au and $d_{Sn\leftarrow O} = 2.912$ Å for **4**, and $\delta V = 0.49$ au and $d_{Sn\leftarrow O} = 2.601$ Å for **3**.

In a solid-state system, the EFG at the site of a given ^{119}Sn nucleus will be affected not only by its ligands but also by other neighboring molecules. Therefore, it seems reasonable to consider supramolecular moieties consisting of two, three, or more molecules (which will be referred to sometimes as dimer, trimer, etc. for the sake of brevity) until the EFG at the probe tin atom reflects the real solid-state environment of that atom. Figure 1 shows the experimental quadrupole splitting (Δ_{exp}) values (horizontal lines in the inserts) versus calculated V values obtained for the probe tin atom situated in the center of the actual supramolecular moiety (see also Table 3). In other words, each horizontal line represents one particular compound and the individual points along each horizontal line represent different supramolecular moieties with the monomers (in vacuo and nonoptimized crystal structure) to the far right for compounds **3**−**5** and to the far left for **1**. The V_{calc} values corresponding to the optimized gas-phase structure and to the nonoptimized monomer taken from the solid-state structure are clearly separated from the rest. The points belonging to increasingly larger supramolecular moieties seem to approach a limit and to oscillate about it. Even if this convergence cannot be mathematically described, it can be expected that beyond a

TABLE 3: Calculated Values of the Quantity *V* and the Quadrupole Splitting Δ_{calc} Obtained for the Central Tin Atom in Different Supramolecular Moieties of Compounds 1−5

size of supramolecular moiety[a]	V[b]	Δ_{calc}[b]
Compound **1**		
3	4.32	4.01
5	4.33	4.03
7	4.37	4.06
9	4.34	4.03
13	4.34	4.04
Compound **2**		
1[c]	−2.00	−1.86
1[c]	−1.66	−1.55
2	−2.06	−1.92
3	−2.05	−1.91
4	−2.11	−1.96
6	−2.13	−1.98
7	−2.05	−1.90
Compound **3**		
2	−3.27	−3.04
3	−3.43	−3.19
4	−3.49	−3.24
5	−3.51	−3.26
6	−3.52	−3.27
Compound **4**		
2	−3.03	−2.82
3	−3.13	−2.91
4	−3.18	−2.96
12	−3.21	−2.98
Compound **5**		
2	−2.85	−2.65
3	−3.25	−3.02
6	−3.39	−3.16
9[d]	−3.52	−3.28
9[d]	−3.59	−3.34
27	−3.47	−3.23

[a] The number of molecules composing the supramolecular moiety (e.g., 3 means a trimer). [b] For the calculation of Δ (mm s^{-1}) from the value of *V* (au), the calibration curve proposed by Barone et al.[9] was used (with the calibration factor 0.93 mm s^{-1} au^{-1}). [c] For compound **2**, all molecules (two molecules per asymmetric unit) of all known polymorphs (CSD[16] codes: TPSNCL01, TPSNCL02, TPSNCL03) were considered; however, the *V* values found were very similar, so only the two limits of the range are shown here. [d] For compound **5**, two different supramolecular moieties consisting of nine molecules were considered (see Figure 5b).

certain size of the supramolecular moiety, V_{calc} will have a certain limiting value.

To decide which *V* value is the closest to the limit, a calibration is needed. Figure 1 shows four calibration curves obtained from four different values of *Q* found in the literature (see Table 2 for details). Two values (Q_1 and Q_3) were obtained by relativistic[12] and nonrelativistic[9] DFT(B3LYP) methods; the full-potential linear-muffin-tin-orbitals (FP-LMTO) method within the local-density approximation (LDA) to DFT resulted in another estimate (Q_2).[4a] As the calculated value of *Q* is model-dependent, the calibration curve obtained from a computation at the nonrelativistic DFT(B3LYP) level[9] is the most suitable one for the present work, where the same method was used.

Returning to Figure 1, compound **2** deserves particular attention since the series of *V* values obtained for the ^{119}Sn core of increasingly larger supramolecular moieties does not seem to converge to the value estimated from the calibration curve. Actually, the difference is quite significant (Figure 1). An explanation for this discrepancy will be given in section 3.6 after the individual analysis of the other four compounds.

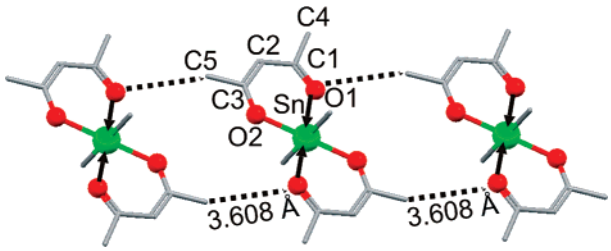

Figure 2. Trimeric supramolecular moiety and molecular structure of compound **1**.[27] H atoms are omitted for clarity. The bond distance Sn ← O1 is longer than Sn−O2. This may be a consequence of weak C−H···O intermolecular interactions because of the relatively short C5−O1 distances shown by dashed lines.

3.2. $Me_2Sn(acac)_2$ (1). The compound bis(2,4-pentanedionato)dimethyltin(IV), or $Me_2Sn(acac)_2$ (where acac denotes acetylacetonato ligand), has been subject to numerous studies concerning its molecular structure both in different solutions and in the solid state. On the basis of infrared and Raman spectra together with ^{1}H NMR ($CDCl_3$ solution), McGrady and Tobias[24] concluded that this complex has a *trans*-Me_2 structure both in solid state and in solution. All Mössbauer measurements indicated *trans*-Me_2 in the solid state,[1,17,25,26] and the partial quadrupole splitting model also supported this arrangement: $\Delta_{calc} = 4.12$ mm s^{-1} compared to the experimental value of $\Delta_{exp} = 4.02$ mm s^{-1}.[17]

Miller and Schlemper confirmed the trans configuration of **1** by determining its crystal structure.[27] They found that the C−Sn−Cl angle is exactly 180° and that the maximum deviation of any ligand atom from the least-squares plane defined by them is 0.03 ± 0.02 Å indicating no significant deviation from planarity. Thus, the tin atom shows an almost perfect octahedral configuration. The bond distances (Me)C1−C2(H) and (Me)-C3−C2(H) in the ligand are significantly different (1.438 Å and 1.365 Å) without obvious chemical reason (Figure 2). (The bond distances are expected to be identical because of the electron delocalization in the chelate ring.) The calculated gas-phase structure reflects the expected symmetrical octahedral geometry. The single (Me)C−C(H) distance (1.408 Å) is nearly equal to the average of the two different (Me)C−C(H) distances (1.365 Å and 1.438 Å) found in the solid-state structure. However, at the supramolecular level, weak intermolecular C5−H···O1 bonds (Figure 2) may occur because of the relatively small C5−O1 intermolecular distance ($d = 3.608$ Å) and these interactions may explain the asymmetry in the chelate ring. This hypothesis seems to be supported by the fact that the calculated Δ_{calc} (4.01 mm s^{-1}) obtained for a trimeric moiety associated via this bonding is very close to the experimentally determined value (Tables 1 and 3). At the same time, the weakness of this interaction is demonstrated by the narrow range of the calculated *V* values from 4.25 to 4.37 au.

3.3. Me_3Sn-succinimide (3). *N*-(Trimethylstannyl)succinimide crystallizes as a flattened helical polymer, which completes its rotation with every fifth molecule.[20] In this coordination polymer, the nearly planar trimethyltin units are axially bridged by one ←O=C−N− linkage of succinimide ligand. This intermolecular contact completes the coordination sphere of tin, increasing its coordination number from four to five. There are two crystallographically independent molecules per asymmetric unit (**3A** and **3B**). In molecule **3A** (Figure 3a), one methyl group is in the plane of the succinimide ring, and in molecule **3B**, (Figure 3b) all three methyl carbons are out of this plane.

Geometry optimizations, starting both from **3A** and **3B**, resulted in a single gas-phase structure, which is similar to **3A** but the geometry around the tin atom is closer to a distorted

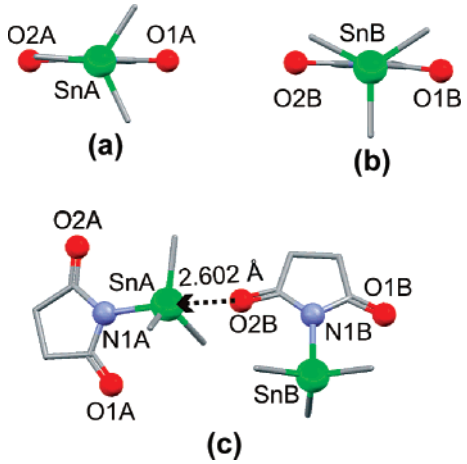

Figure 3. (a) Form A of compound **3** (**3A**). (b) Form B of compound **3** (**3B**). (c) Molecules **3A** and **3B** are linked via intermolecular Sn ← O bonding.[20] H atoms are omitted for clarity.

tetrahedron. The quadrupole splitting calculated for this structure, −2.44 mm s^{-1}, is significantly different from the values calculated for the solid-state monomers (without optimization), for example, −2.89 mm s^{-1} for **3A**. (The difference between the Δ_{calc} values for **3A** and **3B** is small, 0.07 mm s^{-1}, so only the value calculated for **3A** is shown in Table 1.) Furthermore, all calculated values are far from the experimental value, Δ_{exp} = 3.14 (±0.06) mm s^{-1}.[20] Calculation for two neighboring molecules linked by an intermolecular Sn ← O contact of 2.602 Å (Figure 3c) gives a somewhat closer value, −3.04 mm s^{-1}, to that of the isolated monomer (see Table 3). Increasing the size of the supramolecular moiety considered to a trimer results in a Δ_{calc} value of −3.19 mm s^{-1}, which is in good agreement with the measured value.[20] Supramolecular moieties of four, five, and six molecules have also been considered (see Table 3), and the values of Δ_{calc} increased slightly (3.24, 3.26, and 3.27 mm s^{-1} for a supramolecular moiety of 4, 5, and 6 molecules, respectively); however, these differences are negligible when considering the assumed computational error.

3.4. Me_3Sn-phthalimide (4). At a molecular level, the complex *N*-(Trimethylstannyl)phthalimide is very similar to its succinimide analogue. Only one of the carbonyl oxygens of phthalimide participates in an intermolecular bonding with a neighboring tin atom.[28] However, the asymmetric unit of the former complex contains only one molecule, which is similar to **3B** (Figure 3b): the three methyl groups are roughly planar and out of the phthalimide ring plane. Because of the Sn ← O intermolecular interaction (the Sn−O distance is 2.912 Å), the two O=C−N parts of the ring are slightly asymmetric (the bond ←O=C is 1.195 Å, while the other one is 1.178 Å) and the geometry around tin is distorted toward a trigonal bipyramidal structure with average bond angles C−Sn−C and C−Sn−N of 116.9° and 100.0°, respectively. In the gas-phase structure, the geometry at tin is closer to tetrahedral (the average C−Sn−C and C−Sn−N angles are 113.0° and 105.7°, respectively) and the two O=C−N moieties are identical, with a C−O distance of 1.219 Å. Despite the structural similarities with the succinimido complex, compound **4** aggregates in a completely different fashion. While **3** associates in infinite helical chains propagating along its crystallographic axis *b*, compound **4** forms discrete, tetrameric moieties (Figure 4a) organized in parallel layers defined by the *a* and *b* axis (Figure 4b). The Mössbauer parameters of this compound were redetermined in the present work, and the absolute value of the quadrupole splitting was found to be $|\Delta_{exp}|$ = 2.92 mm s^{-1}, in contrast to the previously

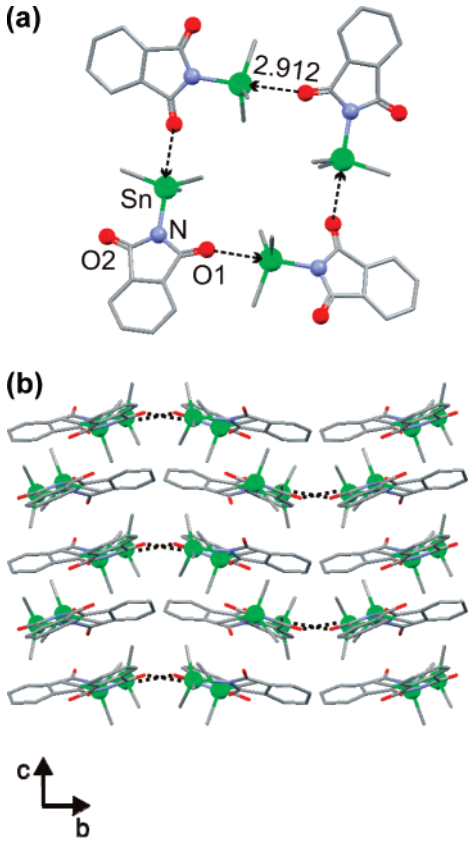

Figure 4. (a) Compound **4** forms tetrameric supramolecular moieties in the solid state. Molecules are linked by Sn ← O bonds.[28] H atoms are omitted for clarity. (b) The tetrameric supramolecular moieties (intermolecular Sn−O bonds are shown by dashed lines) are organized in parallel layers along the crystallographic axis *c*.

reported value of 3.22 mm s^{-1}.[21] The difference between the values found by Gassend et al. and that of the present work is not surprising, since a difference of the same order was also found in the case of compound **3** (Table 1).

The Δ_{calc} values at the optimized gas-phase and the nonoptimized solid-state monomer structures, −2.41 mm s^{-1} and −2.63 mm s^{-1}, respectively, are again very different from the experimental value (Table 1). If two neighboring monomers are considered as a dimer, then the quadrupole splitting calculated (−2.82 mm s^{-1}) for the tin atom involved in the intermolecular contact gives a better estimate of the experimental value (Table 3). Adding a third molecule to the dimer results in −2.91 mm s^{-1} for the tin situated in the center of this trimer. However, addition of further molecules to the supramolecular moiety considered increases slightly the estimated values of the EFG at the central tin nuclei (Table 3), but the value of Δ_{calc} (−2.98 mm s^{-1}) found for a supramolecular moiety of 12 molecules (tetrameric supramolecular moiety and four adjacent molecules from the upper and from the lower layer) is not significantly different from the value obtained for a trimer.

3.5. Me_3SnCl (5). In the gas phase, trimethyltin chloride shows a pseudo-C_{3v} structure, which is unaffected by the influence of any intermolecular interaction or packing forces. All three C−Sn−Cl and C−Sn−C bond angles are identical (105.5° and 113.1°, respectively), and the same value (2.137 Å) is found for the three Sn−C bond lengths, too. This symmetry is also reflected by the obtained Mössbauer parameters: η = 0 and Δ_{calc} = −2.17 mm s^{-1}, typical values for tetrahedral trimethyltin(IV) compounds of the type Me_3SnL, where L is a monovalent ligand.[17] In the solid state, the monomer becomes even more distorted from the ideal tetrahe-

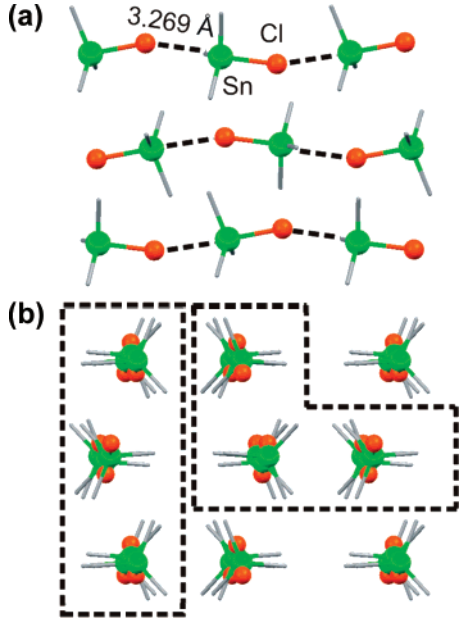

Figure 5. (a) Crystal structure of compound **5** formed by zigzagging polymeric chains bonded through intermolecular Sn···Cl bridges.[29] (b) Supramolecular moiety of 27 molecules. The polymeric chains are perpendicular to the plane of the sheet. Dashed frames group two different supramolecular moieties of nine molecules (three parallel trimers) considered in the calculations.

dral symmetry. For example, the C−Sn−C angle opens from 113.1° in the C_{3v} structure to 117.1° (mean) in the structure obtained from single-crystal X-ray diffraction.[29] This distortion toward a trigonal bipyramidal structure is due to the weak coordination of the chlorine atom that belongs to a neighboring Me_3SnCl molecule. The intermolecular Sn···Cl interaction results in polymeric chains composed of quasi-planar trimethyltin(IV) units bridged by chlorine atoms at unequal distances (the intramolecular Sn−Cl and the intermolecular Sn···Cl distances are 2.430 and 3.269 Å, respectively). The chains are nearly linear at tin, the Cl−Sn−Cl angle is 176.8° but is bent at the chlorine (the Sn−Cl···Cl angle is 150.3°) giving a zigzag form to the polymeric backbone (Figure 5a).

These intermolecular interactions have to be taken into account when calculating the EFG for compound **5**. First, a dimeric and then a trimeric supramolecular moiety was considered. The Δ_{calc} values obtained are −2.65 and −3.02 mm s^{-1}, respectively, while the experimental value is $\Delta_{exp} = -3.32 \pm 0.03$ mm s^{-1} (Table 3).[22] Even if the shortest interchain tin−chlorine contact distances are greater than the sum of the tin and chlorine van der Waals radii (3.85 Å),[30] the EFG at a given tin atom seems to be affected by molecules in the neighboring chains. Taking two parallel trimers gives a Δ_{calc} value of −3.16 mm s^{-1}, and thus it is still insufficient to reproduce the EFG that would explain the experimental Δ_{exp} value. Two different supramolecular moieties of nine molecules (three parallel trimers) were then considered (Figure 5b), and both supramolecular moieties result in Δ_{calc} values (−3.28 and −3.34 mm s^{-1}) very similar to the experimental one. Increasing the number of trimers to nine and forming a supramolecular moiety of 27 molecules (Figure 5b) did not notably affect the results (Table 3).

3.6. Ph_3SnCl (2), the Exception. As mentioned above, compound **2** seems to be an exception in the sense that even if a supramolecular moiety of six or seven molecules is considered, the largest value obtained for $|\Delta_{calc}|$ is only 1.98 mm s^{-1} (Table 3), which is significantly smaller than the experimental values of 2.51−2.61 mm s^{-1}.[18,19]

Because of its large quadrupole splitting, the structure of compound **2** was subject to several controversial studies. Some authors[2,31,32] concluded that compound **2** must be weakly associated, because such a large Δ value for a monomeric four-coordinate molecule would require unrealistically large distortion from the tetrahedral structure. Others[3,33,34] suggested that steric effects of the bulky phenyl groups prevent intermolecular association via chlorine bridges and that the large Δ value is only a consequence of distortions from tetrahedral geometry. The first crystal structure of compound **2** was published in 1970,[35] and it indicated that it is tetrahedral at room temperature. Afterward, on the basis of the study of 37 triphenyltin compounds, Poller and Ruddick[19] stated that even if it is four-coordinate at room temperature, at 80 K the structure must be trigonal bipyramidal. Bancroft and co-workers[18] tried to elucidate this problem by comparing the Mössbauer spectrum at 80 K to that obtained at 110 and 295 K, and the Δ_{exp} values found were 2.54 and 2.46 mm s^{-1}, respectively. They concluded that the differences between these values and that for 80 K (2.61 mm s^{-1})[19] are not significant, so compound **2** appears to be four-coordinate at both high and low temperatures. Molloy and Quill[36] made a tentative classification of the structures of triphenyltin compounds on the basis of variable-temperature Mössbauer measurements. They tried to identify lattice type (monomeric or different polymers) of triphenyltin compounds of unknown X-ray structure by comparing their Mössbauer parameters with those of triphenyltin compounds of known crystal structure. According to the results of previous crystallographic analysis,[35] the solid-state structure of Ph_3SnCl was taken as a reference to monomeric compounds. Finally, Harris and Sebald[37] compared chemical shifts obtained from solution ^{119}Sn-NMR and solid-state ^{119}Sn CP/MAS NMR spectra. They found a very small difference (10 ppm) for compound **2**, so they concluded that no association occurs in the solid state. However, they came to the same conclusion with **6**, because the difference in the chemical shifts proved to be very similar (15.8 ppm), although its crystal structure shows weak Sn···Cl interactions.

For the large experimental quadrupole splitting value found for compound **2**, several explanations can be envisaged: (a) the polymorphic modifications studied by X-ray diffraction and Mössbauer spectroscopy were different; (b) the pressure applied on the sample may have induced a reorganization of the molecules in the solid state; and (c) cooling the compound to 80 K to perform low-temperature Mössbauer measurements may have affected the structure. These possibilities will be discussed in detail below.

(a) Polymorphism. Because of the complex interactions between the phenyl rings, both CH···π and $\pi-\pi$ stackings, and their low rotational barrier, compounds containing triphenyltin(IV) group tend to form different polymorphs.[38] This is also the case with triphenyl-tin chloride (**2**). A search of the Cambridge Crystallographic Structural Database (CSD)[16] for this compound resulted in four structures with the following CSD codes: TPSNCL,[35] TPSNCL01[39] (redetermination of the former structure), TPSNCL02,[39] and TPSNCL03.[40] These structures represent three different polymorphic forms of compound **2**. The structural differences are not substantial and, as a consequence, the calculated Δ_{calc} values are very similar (Table 3). Therefore, polymorphism cannot explain the deviations of the Δ_{calc} values from their experimental counterparts. In addition, the Mössbauer measurements were performed in different

laboratories, but still the results obtained for different samples were quite similar, so it seems very unlikely that the sample used was an unknown polymorph.

(b) Effect of Pressure. Warner et al.[41] examined the effect of pressure on the vibrational spectra of the tetraphenyl Group 14 compounds, Ph_4M (M = Si, Ge, Sn, Pb). For all four compounds, they found a structural transition most probably associated with phenyl-ring rotations. Pressure-tuning Raman and infrared spectra were measured for $(o\text{-}CH_3C_6H_4)_3SnNCS$ by Xu et al.[42] who also detected a phase transition. These compounds are essentially tetrahedral, and at ambient pressure, all the nonbonding distances are longer than the sum of the van der Waals radii of the atoms concerned, so there appears to be no steric strain in their solid-state structure. When increasing the pressure, the volume of the unit cell decreases. The steric strain thus induced can be readily accommodated by slight phenyl ring rotations. The relative mobility of the phenyl groups was also indicated by the gradual change with pressure. However, the phase transition occurred in each case at pressures higher than 10 kbar, which means that such a change in the structure cannot be induced without a deliberate pressure application. In summary, the pressure effect cannot furnish an explanation for the difference between the measured and the calculated Δ values.

(c) Phase Transition due to the Change in Temperature. It must be stressed that Mössbauer measurements on organotin(IV) compounds are generally performed at low temperature (~80 K), whereas in most cases the crystal structures are determined at room temperature (~295 K). However, the actual structure may be slightly different at these temperatures. The best-established organotin example is tri(cyclohexyl)tin chloride ($cHex_3SnCl$, **6**). Asadi et al.[43] carried out a detailed study of this compound by determining its structure at nine different temperatures between 108 and 298 K. Their work revealed that with decreasing temperature the Sn−C and Sn−Cl bond distances increase from 2.151 Å to 2.169 Å and from 2.415 Å to 2.466 Å, respectively. The average bond angle C−Sn−C opens from 116.9° to 118.2°, while the average C−Sn−Cl angle decreases from 100.3° to 97.7°. These changes in molecular parameters show a general distortion from essentially tetrahedral to trigonal bipyramidal geometry about tin, which is accompanied by the decrease of the intermolecular Sn···Cl distance from 3.298 Å to 3.008 Å. In summary, as the temperature decreases, the Sn···Cl interactions strengthen and the intramolecular Sn−Cl interactions weaken. The authors noted that at about 248 K a disorder−order transition from space group $P2_1/m$ (at high temperatures) to $P2_1/c$ (at low temperatures) takes place. Beckmann et al.[44] observed a similar disorder in the structure of $(Me_3SiCH_2)_3SnF$ and its chloride analogue determined at 291 K. On the basis of single-crystal X-ray analysis and spectroscopic studies, they found that these compounds show a structure between the polymeric and monomeric forms with a [4 + 1]-coordinated tin atom. Results of their ab initio MO calculations indicated that the equilibrium angle of Sn−X···Sn (X = F, Cl) linkages is 180° and that they are highly flexible. These characteristics were found by Gillespie[45] to be indicative of highly ionic Sn−X bonds. To elucidate the reason of the disordered structures, Beckmann et al. evaluated the energy profiles for the motion of the fluorine atoms from one tin to another.[44] The potential energy surface scans were performed at fixed Sn−Sn separations. They found that at small Sn−Sn distances the energy profile resembles a parabola (with one minimum at the halfway point), whereas at very large Sn−Sn separations they obtained double-minimum potential curves, where the fluorine atoms are trapped in their respective potential wells. However, for reasonably small Sn−Sn separations, the energy barrier between the two wells is low enough to allow the fluorine atoms to oscillate between the two minima. The disorder found for compound **6** may be explained by interpretations of these results. On cooling, the difference between the intra- and intermolecular Sn−Cl distances decreases and the coordination geometry at tin moves toward trigonal bipyramidal. According to the reinterpretation of the nature of element−halogen bonds made by Gillespie,[45] this means that the Sn−Cl bonds in **6** become more ionic. The disorder that occurred between 298 and 223 K may be indicative of two potential wells separated by a low-energy barrier, which allows an oscillating motion of the chlorine atoms between their tin neighbors.

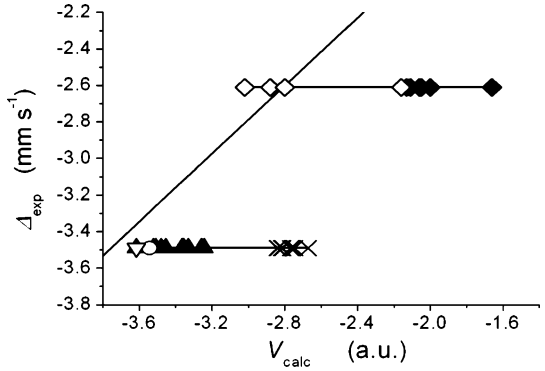

Figure 6. Experimental quadrupole splitting values (Δ_{exp}) of compounds **2** and **6** are plotted against the V_{calc} values calculated for different supramolecular moieties. Lower horizontal line: monomeric (−×−) and trimeric (▲) supramolecular moieties for the nine structures of **6** corresponding to nine different temperatures (108−298 K) as well as one supramolecular moiety of five molecules (▽) and the extrapolated structure to 80 K (○). Upper horizontal line: selected values (see Table 3) for compound **2**; the value for the in vacuo structure is represented by the right-most full rectangle (♦) of the series. Models of **2** at 80 K (◇) created from trimeric supramolecular moieties of compound **6** give the expected *V* values corresponding to the experimental quadrupole splitting value.

As the intermolecular interaction plays an important role in the structure of **6**, the calculation of the quadrupole splitting value for a monomer is not expected to provide a good accordance with the experimental value of (−)3.49 mm s^{-1} [43] (Figure 6), so trimeric supramolecular moieties were also considered (Table 4). For the structure determined at the lowest temperature (108 K), the central tin of a supramolecular moiety of five molecules gave $\Delta_{calc} = -3.36$ mm s^{-1}. Below the transition temperature of 248 K, the quadrupole splitting seems to follow the changes in the molecular parameters in a quasi-linear way (Figure 7).

These results for compound **6** suggest that a similar phenomenon may occur in the case of triphenyltin chloride, that is, the coordination geometry around tin becomes more distorted from pseudo-tetrahedral toward pseudo-trigonal bipyramidal, and this could be reflected in the relatively large value of the measured Δ_{exp}. This means that with the progressive distortion of the known structure of compound **2**, the calculated Δ_{calc} should approach the experimental value. The structure correlation method[46] applied to organotin compounds[47] could indicate an appropriate pathway to the distortion. The examination of 55 four- and five-coordinate R_3SnCl (R = aryl, alkyl) crystal structures found from a search of the CSD provided for us the structural data used to establish the correlation function (see eq 7) driving the distortion procedure. The constant values (2.318

TABLE 4: Calculated *V* Values and the Quadrupole Splittings (Δ_{calc}) Obtained for Monomers and Trimers of Compound 6[e]

CSD code[a]	V[b]	Δ_{calc}[b]
Compound **6**		
Monomers		
CTPHSN01 (298 K)	−2.66	−2.48
CTPHSN02 (273 K)	−2.67	−2.49
CTPHSN03 (248 K)	−2.76	−2.57
CTPHSN04 (223 K)	−2.74	−2.55
CTPHSN05 (198 K)	−2.77	−2.58
CTPHSN06 (173 K)	−2.81	−2.61
CTPHSN07 (148 K)	−2.82	−2.62
CTPHSN08 (123 K)	−2.83	−2.63
CTPHSN09 (108 K)	−2.84	−2.64
Trimers		
CTPHSN01 (298 K)	−3.24	−3.01
CTPHSN02 (273 K)	−3.26	−3.03
CTPHSN03 (248 K)	−3.35	−3.12
CTPHSN04 (223 K)	−3.33	−3.10
CTPHSN05(198 K)	−3.36	−3.13
CTPHSN06 (173 K)	−3.45	−3.21
CTPHSN07 (148 K)	−3.48	−3.23
CTPHSN08 (123 K)	−3.51	−3.26
CTPHSN09 (108 K)	−3.52	−3.27
structure extrapolated to 80 K	−3.54	−3.29
Supramolecular Moiety of Five Molecules		
CTPHSN09 (108 K)	−3.61	−3.36
Compound **2**[c]		
Monomer		
CTPHSN01[d]	−2.16	−2.01
Trimers		
CTPHSN09	−3.02	−2.81
CTPHSN04	−2.88	−2.68
CTPHSN01	−2.80	−2.60

[a] The codes refer to the structures of **6** determined at different temperatures (in parentheses). [b] For the calculation of Δ (mm s^{-1}) from the value of V (au), the calibration curve proposed by Barone et al.[9] was used (with the calibration factor 0.93 mm s^{-1} au^{-1}). [c] For modeling the possible intermolecular interactions in compound **2** (at 80 K), the calculations were performed on known crystal structures (CTPHSN01, 04, and 09) of **6**, but the original cyclohexyl ligands were replaced by phenyl rings. [d] Results for a monomer are shown here to compare the value obtained for a trimeric supramolecular moiety of the same structure (CTPHSN01 with Ph ligands). [e] Each different CSD code (CTPHSN01-09) corresponds to a structure of **6** determined at a different temperature.

and 0.83) were obtained from the correlation plot of the Sn−Cl bond distances versus log[(1 − 3 cos(C−Sn−Cl)$_{ave}$)/2] (Figure 8).

$$d(\mathrm{Sn{-}Cl})/\text{Å} = 2.318(\pm 0.003) - 0.83(\pm 0.02)\log[(1 - 3\cos(\mathrm{C{-}Sn{-}Cl})_{ave})/2] \quad (7)$$

The example of compound **1** showed that if the intermolecular interactions are not significant, then Δ_{calc} calculated for a single molecule from the crystal gives a good approximation of the experimental value. Thus, if the distortion of compound **2** is an inherent property of the Ph_3SnCl molecule and not a result of any intermolecular interaction, then the calculated Δ_{calc} for a monomer should be relevant. Table 5 shows the molecular parameters of the monomer Ph_3SnCl in each step of the distortion and the Δ_{calc} values obtained for each geometric variant.

As expected, the calculated Δ_{calc} values increase with the distortion of the molecule, but, even in the fifth step, the

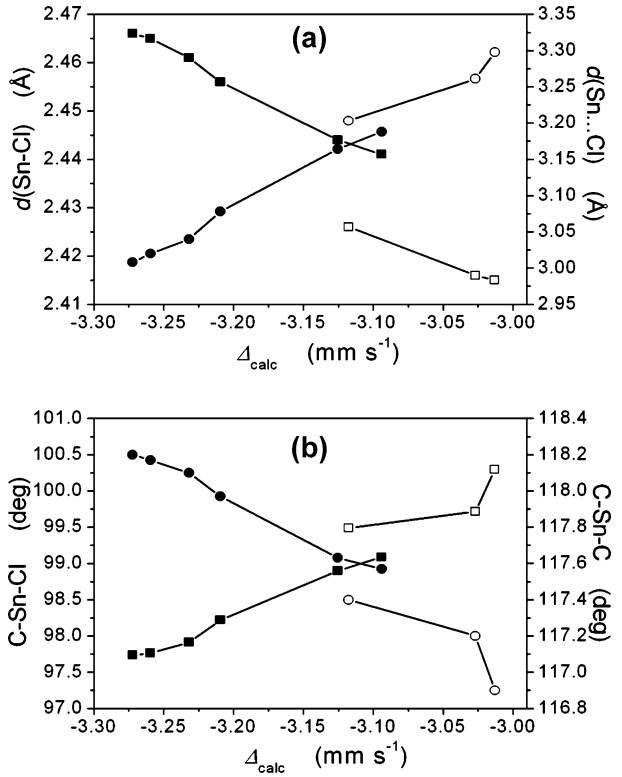

Figure 7. (a) Intramolecular Sn−Cl (● and ○) and intermolecular Sn···Cl (■ and □) distances for different structures of **6** plotted as a function of the calculated quadrupole splittings (Δ_{calc}). At low temperatures (108−223 K), a quasi-linear relation is observed (● and ■). Discontinuity between the parameters corresponding to the structures determined at 248 and 223 K reflects the phase transition described by Asadi et al.[43] (b) Average C−Sn−Cl (● and ○) and C−Sn−C (■ and □) angles for the nine different structures of **6** plotted as a function of the calculated Δ_{calc} values. Full symbols (● and ■) refer to low temperatures (108−223 K), and open symbols (○ and □) refer to higher temperatures (248−298 K).

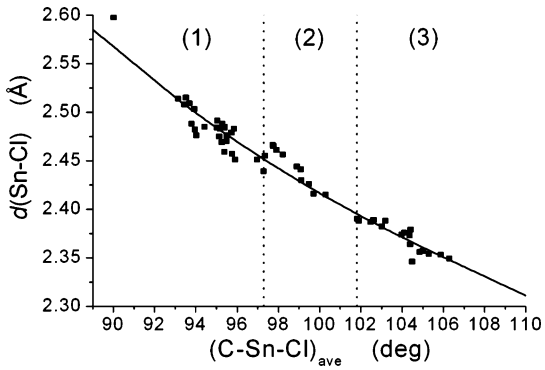

Figure 8. Correlation plot of Sn−Cl bond distances versus average C−Sn−Cl angles in R_3SnCl (R = alkyl, aryl) compounds found in the CSD.[16] The curve defined by eq 7 is fitted to these plots. Regions 1 and 3 correspond to five- and four-coordinate tin compounds, respectively. The intermediate region 2 contains tin compounds participating in weak intermolecular interaction with a coordination number between four and five.

calculated value is much smaller (2.28 mm s^{-1}) than the experimental value (2.51−2.61 mm s^{-1}) though the geometry at this step is typical of five-coordinate organotin compounds (Figure 8). This means that obtaining a larger quadrupole splitting is only possible if a Sn···Cl intermolecular interaction is taken into account. To verify this hypothesis, several crystal structures from the CSD search have been considered, where tin participates in an intermolecular interaction with an adjacent

TABLE 5: Distortion of Compound 2 According to Eq 7; Relevant Molecular Parameters and the Calculated Quadrupole Splitting (Δ_{calc}) Values for Each Step

step[a]	$(C-Sn-Cl)_{ave}$[b]	$d(Sn-Cl)$[b]	V[c]	Δ_{calc}[c]
1	105.0	2.361	−2.01	−1.86
2	103.0	2.382	−2.11	−1.96
3	101.0	2.405	−2.22	−2.07
4	99.0	2.429	−2.36	−2.20
5	97.0	2.456	−2.45	−2.28

[a] Step-by-step distortions were carried out on the original structure of compound **2**. The form TPSNCL02 was taken initially. [b] Relevant molecular parameters, the average C−Sn−Cl angle (deg) and the Sn−Cl bond length (Å), are shown. [c] For the calculation of Δ (mm s^{-1}) from the value of V (au), the calibration curve proposed by Barone et al.[9] was used (with the calibration factor 0.93 mm s^{-1} au^{-1}).

chlorine atom. The original aryl/alkyl ligands were replaced by phenyl rings, and the molecular parameters (bond lengths and angles) around tin were left unchanged. The Δ_{calc} values were computed on these model structures. A series derived from different modifications of **6** is only presented here, because it illustrates well the effect of intermolecular interactions on the calculated quadrupole splitting of the Ph_3SnCl models (Table 4).

The best accordance with experimental values (Figure 7) is obtained for the structure CTPHSN01 (see footnote c of Table 4). In this structure, the intermolecular Sn···Cl distance is 3.298 Å, which cannot be an indication of a significant interaction[43] but which is considerably shorter than the sum of the van der Waals radii (3.85 Å[30]) of tin and chlorine, so it can have an important contribution to the EFG. This is also reflected by the fact that the Δ_{calc} value, −2.01 mm s^{-1}, obtained for the monomer is just slightly larger than those found for all supramolecular moieties (dimer, trimer, etc.) of compound **2** (Table 4). When a stronger intermolecular interaction takes place, for example, $d_{Sn\cdots Cl}$ of 3.188 Å for CTPHSN04 and 3.008 Å for CTPHSN09, the Δ_{calc} values obtained are too large compared to the experimental ones, which makes it rather unlikely that a Sn···Cl distance is shorter than 3.298 Å. Finally, according to our calculations, at low temperature a structural change in the crystal lattice of **2** toward polymeric chains is very probable. In this structure, an intermolecular distance larger than 3.188 Å, but smaller than the sum of the van der Waals radii of tin and chlorine, may explain the large experimental value of the quadrupole splitting found for compound **2**.

4. Conclusions

EFG calculations of compounds **3**−**5** revealed that optimized geometries of isolated molecules are not appropriate to model the electronic environment of the tin nucleus in these compounds. However, inclusion of at least three neighboring molecules in the model leads to much improved predictions for the EFG, resulting in the experimental quadrupole splitting value.

Structural differences due to differences in temperature may be important, especially in compounds where intermolecular interactions occur. The example of compound **6** shows that as the temperature decreases, the bond lengths and bond angles may change until a phase transition takes place. As these modifications are also reflected by the changing value of Δ_{calc}, one has to be careful when X-ray structures obtained at room temperature are considered to explain the experimental Δ value measured at 80 K.

Taking this observation into account, we explained the origin of the large value of the quadrupole splitting obtained for compound **2**. Computational analysis showed that such a large splitting is only possible if distortions of the molecular structure from tetrahedral geometry are accompanied by the formation of weak intermolecular interactions. In contrast to the known structure of **2**, if the intramolecular Sn−Cl bond is set to 2.415 Å, the C−Sn−Cl angle to 100.0°, and the intermolecular Sn···Cl distance to 3.298 Å, the Δ_{calc} value calculated for a supramolecular moiety consisting of three molecules of Ph_3SnCl approximatively equals the experimental value. These results raise again the question about the structure of Ph_3SnCl at 80 K.

Acknowledgment. We gratefully acknowledge financial support from the Hungarian Scientific Research Fund (OTKA K67835, T047185, and T049815).

Supporting Information Available: Table S1 calculated eigenvalues (V_{xx}, V_{yy}, and V_{zz}) and asymmetry parameters (η) for each calculation; Table S2 relevant geometric parameters of compounds used to establish the correlation function given by eq 7; calculated atomic coordinates of all optimized molecules. This material is available free of charge via the Internet at http://pubs.acs.org.

References and Notes

(1) Parish, R. V.; Platt, R. H. *J. Chem. Soc. A* **1969**, 2145−2150.
(2) Parish, R. V.; Platt, R. H. *Inorg. Chim. Acta* **1970**, 65−72.
(3) Clark, M. G.; Maddock, A. G.; Platt, R. H. *J. Chem. Soc., Dalton Trans.* **1972**, 281−290.
(4) (a) Svane, A.; Christensen, N. E. *Phys. Rev. B* **1997**, *55*, 12572−12577. (b) Blaha, P.; Schwarz, K.; Faber, W.; Luitz, J. *Hyperfine Interact.* **2000**, *126*, 389−395.
(5) Halkier, A.; Kirchner, B.; Huber, H.; Jaszuński, M. *Chem. Phys.* **2000**, *253*, 183−191.
(6) (a) Gerber, S.; Huber, H. *J. Mol. Spectrosc.* **1989**, *134*, 168−175. (b) Gerber, S.; Huber, H. *Chem. Phys.* **1989**, *134*, 279−285. (c) Eggenberger, R.; Gerber, S.; Huber, H.; Searles, D.; Welker, M. *J. Mol. Spectrosc.* **1992**, *151*, 474−481.
(7) Pavanello, M.; Mennucci, B.; Tomasi, J. *Theor. Chem. Acc.* **2006**, *116*, 711−717.
(8) Rega, N.; Cossi, M.; Barone, V. *J. Chem. Phys.* **1996**, *105*, 11060−11067.
(9) Barone, G.; Silvestri, A.; Ruisi, G.; La Manna, G. *Chem. Eur. J.* **2005**, *11*, 6185−6191.
(10) (a) Becke, A. D. *Phys. Rev. A* **1988**, *38*, 3098−3100. (b) Lee, C.; Yang, W.; Parr, R. G. *Phys. Rev. B* **1988**, *37*, 785−789.
(11) (a) Godbout, N.; Salahub, D. R.; Andzelm, J.; Wimmer, E. *Can. J. Chem.* **1992**, *70*, 560−571. (b) Sosa, C.; Andzelm, J.; Elkin, B. C.; Wimmer, E.; Dobbs, K. D.; Dixon, D. A. *J. Phys. Chem.* **1992**, *96*, 6630−6636.
(12) Krogh, J. W.; Barone, G.; Lindh, R. *Chem. Eur. J.* **2006**, *12*, 5116−5121.
(13) Shcherbakov, V. I.; Stolyarova, N. E.; Dyachkovskaya, O. S.; Chulkova, T. I. *Zh. Obshch. Khim.* **1977**, *47*, 2294−2297.
(14) Frisch, M. J.; Trucks, G. W.; Schlegel, H. B.; Scuseria, G. E.; Robb, M. A.; Cheeseman, J. R.; Montgomery, J. A., Jr.; Vreven, T.; Kudin, K. N.; Burant, J. C.; Millam, J. M.; Iyengar, S. S.; Tomasi, J.; Barone, V.; Mennucci, B.; Cossi, M.; Scalmani, G.; Rega, N.; Petersson, G. A.; Nakatsuji, H.; Hada, M.; Ehara, M.; Toyota, K.; Fukuda, R.; Hasegawa, J.; Ishida, M.; Nakajima, T.; Honda, Y.; Kitao, O.; Nakai, H.; Klene, M.; Li, X.; Knox, J. E.; Hratchian, H. P.; Cross, J. B.; Bakken, V.; Adamo, C.; Jaramillo, J.; Gomperts, R.; Stratmann, R. E.; Yazyev, O.; Austin, A. J.; Cammi, R.; Pomelli, C.; Ochterski, J. W.; Ayala, P. Y.; Morokuma, K.; Voth, G. A.; Salvador, P.; Dannenberg, J. J.; Zakrzewski, V. G.; Dapprich, S.; Daniels, A. D.; Strain, M. C.; Farkas, O.; Malick, D. K.; Rabuck, A. D.; Raghavachari, K.; Foresman, J. B.; Ortiz, J. V.; Cui, Q.; Baboul, A. G.; Clifford, S.; Cioslowski, J.; Stefanov, B. B.; Liu, G.; Liashenko, A.; Piskorz, P.; Komaromi, I.; Martin, R. L.; Fox, D. J.; Keith, T.; Al-Laham, M. A.; Peng, C. Y.; Nanayakkara, A.; Challacombe, M.; Gill, P. M. W.; Johnson, B.; Chen, W.; Wong, M. W.; Gonzalez, C.; Pople, J. A. *Gaussian 03*, revision C.02; Gaussian, Inc.: Wallingford, CT, 2004.
(15) (a) Hay, P. J.; Wadt, W. R. *J. Chem. Phys.* **1985**, *82*, 270−283. (b) Wadt, W. R.; Hay, P. J. *J. Chem. Phys.* **1985**, *82*, 284−298. (c) Hay, P. J.; Wadt, W. R. *J. Chem. Phys.* **1985**, *82*, 299−310.
(16) Cambridge Structural Database, version 5.27, November 2005, Cambridge Crystallographic Data Centre, Cambridge.

(17) Davies, A. G.; Smith, P. J. In *Comprehensive Organometallic Chemistry, The synthesis, reaction and structures of organometallic compounds*; Wilkinson, G., Gordon, F., Stone, A., Abel, E. W., Eds.; Pergamon,: Oxford, 1982; Vol. 2, pp 523−530.
(18) Bancroft, G. M.; Butler, K. D.; Sham, T. K. *J. Chem. Soc., Dalton Trans.* **1975**, 1483−1486.
(19) Poller, R. C.; Ruddick, J. N. R. *J. Organomet. Chem.* **1972**, *39*, 121−128.
(20) Hahn, F. E.; Dory, T. S.; Barnes, C. L.; Hossain, M. B.; van der Helm, D.; Zuckerman, J. J. *Organometallics* **1983**, *2*, 969−973.
(21) Gassend, R.; Limouzin, Y.; Maire, J. C.; Muttalib, A. K. M. A.; More, C. *J. Organomet. Chem.* **1974**, *78*, 215−220.
(22) Greenwood, N. N.; Gibb, T. C. *Mössbauer Spectroscopy;* Chapman and Hall Ltd.: London, 1971; pp 404−415.
(23) Haas, H.; Menningen, M.; Andreasen, H.; Damgaard, S.; Grann, H.; Pedersen, F. T.; Petersen, J. W.; Weyer, G. *Hyperfine Interact.* **1983**, *15/16*, 215−218.
(24) McGrady, M. M.; Tobias, R. S. *J. Am. Chem. Soc.* **1965**, 1909−1916.
(25) Fitzsimmons, B. W.; Seeley, N. J.; Smith, A. W. *J. Chem. Soc. A* **1969**, 143−146.
(26) Bancroft, G. M.; Sham, T. K. *Can. J. Chem.* **1974**, *52*, 1361−1366.
(27) Miller, G. A.; Schlemper, E. O. *Inorg. Chem.* **1973**, *12*, 677−681.
(28) Chuprunov, E. V.; Tarkhova, T. N.; Korallova, T. Yu; Belov, N. V. *Dokl. Akad. Nauk SSSR (Russ.*) **1978**, *242*, 606−608.
(29) Lefferts, J. L.; Molloy, K. C.; Hossain, M. B.; van der Helm, D.; Zuckerman, J. J. *J. Organomet. Chem.* **1982**, *240*, 349−361.
(30) Bondi, A. *J. Phys. Chem.* **1964**, *68*, 441−451.
(31) Goodman, B. A.; Greenwood, N. N. *J. Chem. Soc. A* **1971**,1862−1865.
(32) Ensling, J.; Gütlich, Ph.; Hassellbach, K. M.; Fitzsimmons, B. W. *J. Chem. Soc. A* **1971**, 1940−1943.
(33) Maddock, A. G.; Platt, R. H. *J. Chem. Soc. A* **1971**, 1191−1195.
(34) Platt, R. H. *J. Organomet. Chem.* **1970**, *24*, C23−C25.
(35) Bokii, N. G.; Zakharova, G. N.; Struchkov, Yu. T. *Zh. Strukt. Khim. (Russ.*) **1970**, *11*, 828−902.
(36) Molloy, K. C.; Quill, K. *J. Chem. Soc., Dalton Trans.* **1985**, 1417−1423.
(37) Harris, R. K.; Sebald, A. *Organometallics* **1988**, *7*, 388−394.
(38) Prince, P. D.; McGrady, G. S.; Steed, J. *New J. Chem.* **2002**, *26*, 457−461.
(39) Tse, J. S.; Lee, F. L.; Gabe, E. J. *Acta Crystallogr., Sect. C* **1986**, *42*, 1876−1878.
(40) Weng, S. Ng, *Acta Crystallogr., Sect. C* **1995**, *51*, 2292−2293.
(41) Warner, S. D.; Butler, I. S.; Wharf, I. *Spectrochim. Acta A* **2000**, *56*, 453−466.
(42) Xu, Z.; Wharf, I.; Butler, I. S. *J. Mol. Struct.* **2006**, *825*, 130−133.
(43) Asadi, A.; Eaborn, C.; Hitchcock, P. B.; Meehan, M. M.; Smith, J. D. *Inorg. Chem.* **2003**, *42*, 4141−4146.
(44) Beckmann, J.; Horn, D.; Jurkschat, K.; Rosche, F.; Schürmann, M.; Zachwieja, U.; Dakternieks, D.; Duthie, A.; Lim, A. E. K. *Eur. J. Inorg. Chem.* **2003**, 164−174.
(45) Gillespie, R. J. *Coord. Chem. Rev.* **2000**, *197*, 51−69.
(46) Bürgi, H. B. *Angew. Chem.* **1975**, *87*, 461−475; *Angew. Chem., Int. Ed. Engl.* **1975**, *14*, 460−473.
(47) Britton, D.; Dunitz, J. D. *J. Am. Chem. Soc.* **1981**, *103*, 2971−2979.